IL NUOVO CIMENTO **45 C** (2022) 83
DOI 10.1393/ncc/i2022-22083-x

COMMUNICATIONS: SIF Congress 2021

The impact of turbulence on ionospheric plasma density irregularities

P. DE MICHELIS

Istituto Nazionale di Geofisica e Vulcanologia - Roma, Italy

received 4 February 2022

Summary. — Our society is becoming increasingly dependent on Global Navigation Satellite Systems (GNSS), such as the global positioning system (GPS), GLONASS and GALILEO. These systems provide an efficient response to the needs of positioning on our planet and are also used by many infrastructures and applications for timing and synchronization. One of the natural factors that most contribute to the malfunction of these systems, leading to a degradation of their performance, accuracy and reliability, is represented by the ionospheric irregularities, *i.e.*, plasma density variations that may affect the electromagnetic signals propagating through them. By using data recorded onboard the ESA's Swarm constellation, the possible dependence of the loss of lock of GPS signals on a specific typology of ionospheric irregularities is assessed. It is shown that ionospheric irregularities characterized by a turbulent nature and extremely high-density fluctuations can lead to malfunctions of GNSS, thus paving the way for new prediction approaches of their adverse effects.

1. – Introduction

Recently, a project entitled "Characterization of IoNospheric TurbulENce level by Swarm constellation (INTENS)", founded by the European Space Agency (ESA), was concluded. The INTENS team, consisting of researchers from two Italian research institutes (INGV and INAF) and one Greek institute (NOA), achieved interesting results by studying the turbulence processes in the ionospheric F2 layer. Here, I will focus on results obtained during INTENS project relative to the scaling properties of the electron density fluctuations in the mid- and high-latitude topside ionosphere. The analysis, carried out on very long dataset consisting of about 4 years of measurements, permitted to better understand the plasma density irregularities, to analyze one of their interesting aspect, that is, their possible turbulence nature, and to assess the possible dependence of the loss of lock of the global positioning system (GPS) signals on the presence of a specific

kind of ionospheric irregularities. Thereby, the analysis permitted to assess the origin of one of the large space weather effects on the Global Navigation Satellite Systems (GNSS) and users. This paper is essentially a review of the results achieved in the project, some of which have been published by the INTENS team in previous papers [1-5].

As every research, also this this one stemmed from the desire to answer to a series of questions that the scientific community has been asking for some years, since the relevance of the GNSS in our society has substantially increased. Nowadays, many critical infrastructures and our economy are dependent on positioning, navigation, and timing services of GNSS, so that our society is vulnerable to damages due to malfunction of these systems. For this reason, one of the priorities in the space weather community is to investigate the occurrence of plasma irregularities in the ionosphere, to understand their features and their generation mechanisms. Indeed, it is known that plasma irregularities are responsible for the disturbance of radio waves, significantly affect the GNSS and, in the worst case, can even cause a loss of lock event, a condition for which a GNSS receiver can no longer track the signal sent by the satellite, with a consequent degradation of the positioning accuracy.

We see then how we can try to answer questions like "Why are GPS signals sometimes weak or even absent? Why do these disturbances sometimes happen against all predictions? Why can not we predict the possible weakening or even loss of a GPS signal correctly?" To start answering these questions it is necessary to consider a specific physical process, turbulence, which is currently not included in the classical ionospheric prediction models. Each of us knows this type of process if for no other reason that there is a multiplicity of phenomena that happen daily around us in which processes of fluid turbulence are clearly observable. The arabesques formed by the smoke of a cigarette or coffee poured into a glass of milk, the swirling motion of a stream or the motion of the meteorological perturbations observed by satellites are only a few of the examples where fluid turbulence is observed. Turbulence processes also characterize the ionospheric environment, that is the region of space surrounding the Earth, creating a sort of interface between the Earth's atmosphere and space. Several studies have shown that the ionospheric plasma can often be in a state of turbulence and that this turbulence regime plays a fundamental role in the generation and dynamics of the ionospheric plasma density irregularities, that is, heterogeneities in the ionospheric plasma density with spatial dimensions from hundreds of kilometers down to meters. They are present in the F region ionosphere at different latitudes and local times [6]. The high-latitude ionosphere is one of those ionospheric regions where intense plasma density irregularities caused by different processes mainly associated with auroral activities and plasma dynamics can be found. The variations of the electric current systems flowing both parallel and perpendicular to the Earth's magnetic field, the plasma convection, the particle precipitation along the magnetic field lines and the thermospheric heating are among the possible mechanisms responsible for the generation of irregularities at different scales. In the past, it has been suggested that these irregularities can cascade from large scales to small scales due to the occurrence of turbulent phenomena. Indeed, phenomena such as the current convective instability and the $\mathbf{E} \times \mathbf{B}$ gradient drift instability can directly or indirectly be capable of producing cascade processes through which smaller size irregularities are generated [7]. In the standard, fluid picture of turbulence, fluctuation energy is injected at large scales, and nonlinear interactions among eddies lead to a cascade of energy from large to small scales. This means that the plasma density fluctuations in the ionosphere are characterized by infinite degrees of freedom which involve many spatial and temporal scales and a nonlinear transfer of energy between the different scales.

2. – Data

To better understand the features of plasma irregularities, to investigate their possible turbulent origin and to understand whether the loss of GPS signals can be related to the crossing of electromagnetic signals of irregularities characterized by a turbulence regime, we use the data collected recently from the constellation of Swarm satellites. Swarm is ESA's first constellation mission for Earth observation. The mission consists of three identical satellites named Alpha, Bravo, and Charlie (A, B and C), which were launched on 22 November 2013 into a near-polar orbit. Swarm A and C form the lower pair of satellites flying side-by-side (1.4° separation in longitude at the equator) at an altitude of 460 km (initial altitude) and at 87.35° inclination angle, whereas Swarm B is cruising at a higher orbit of 510 km (initial altitude) and at 87.75° inclination angle. In this study, measurements of electron density, N_e, at a rate of 1 Hz collected by the Langmuir Probes [8] onboard Swarm A, during a period of four years (from April 2014 to March 2018) are considered. These data are also used to evaluate RODI, which is the standard deviation of the Rate of change Of electron Density (ROD) in a sliding window of fixed size [1, 9, 10]. Lastly, data provided by precise orbit determination (POD) antennas [11] onboard Swarm A are used to determine the total electron content (TEC), *i.e.*, the electron columnar number density. These measurements are used to singled out loss of lock events by looking for interruptions in the TEC time series for a specific GPS satellite [5]. In this way, it is possible to identify the occurrence of loss of lock (LoL) events. These events have different duration: from a few tens of seconds down to a single second. However, a check of loss of lock events whose duration is 1 s, evidences that most of them are most likely due to hardware outages [12] and for this reason they are removed from the dataset, which consequently contains all the observed events longer than 1 s [5].

3. – Method

In order to verify the possible turbulent nature of the electron density fluctuations measured by Swarm, we analyzed the q-th–order structure function $S_q(\tau)$ of the electron density as a function of the time-delay τ, *i.e.*,

$$S_q(\tau) = \langle \mid N_e(t+\tau) - N_e(t) \mid^q \rangle, \tag{1}$$

where N_e is the electron density, t is the time, and $\langle \ldots \rangle$ stands for a statistical average. It is possible to demonstrate that when a signal, in our case the electron density, is characterized by a scale invariance the q-th–order structure functions $S_q(\tau)$ have a power-law behavior as a function of the separation time τ, *i.e.*,

$$S_q(\tau) = \tau^{\gamma(q)}, \tag{2}$$

where $\gamma(q)$ are the scaling exponents of the structure functions. In the case of simple fractal signals these exponents are expected to be a linear function of the moment order q, while in the case of more complex fractal signals they show a departure from such a linear dependence.

The focus is on the first- and second-order scaling exponent. The first-order scaling exponent $\gamma(1)$, also known as Hurst/Hölder exponent (H) [13], quantifies the persistence

or anti-persistent character of the increments. A signal, whose scaling features are characterized by $H < 0.5$ shows an anti-persistent character of its increments, while a signal, whose scaling features are characterized by $H > 0.5$ shows a persistent character of its increments. In other words, long-range correlated signals are characterized by a sign-persistence of its increments ($H > 0.5$), while in the case of anti-persistent increments ($H < 0.5$) we talk about short-range correlated signals. The second-order scaling exponent $\gamma(2)$ provides information on the signal spectral features via the Wiener-Khinchin theorem [14]. It links the spectral features to the Fourier transform of the auto-correlation function, to which the second-order structure function is directly related. In particular, in the case of a temporal signal $f(t)$ displaying scaling features characterized by a scaling exponent $\gamma(2)$ for the second-order structure function, the power spectral density (PSD) is expected to satisfy the following power-law:

$$PSD(f) \sim f^{-\beta}, \tag{3}$$

where

$$\beta = \gamma(2) + 1. \tag{4}$$

This means that $\gamma(2)$ permits us to know indirectly the spectral characteristics of the analyzed time series allowing us to obtain information on the possible physical processes that cause the observed fluctuations. In fact, spectral characteristics may suggest the different types of instability or turbulence processes that give rise to the observed fluctuations. While for simple mathematical signals the scaling features are generally global, for real signals these properties can acquire a local character due to their inherent spatio-temporal nonstationarity. This is what happens in the case of satellite observations because the satellite crosses different regions observing physical situations that can change in space and time. Thus, in order to apply the structure function analysis to analyze turbulent fields on a local scale it is necessary to implement it on overlapping moving windows and to remove possible large-scale variations that can affect the correct estimation of the scaling features. This approach is known as detrended structure function analysis [1, 3, 15, 16]. This is accomplished by removing a polynomial trend within a window size T before calculating the increment. By doing so, scales larger than T are expected to be removed or constrained and the method acts as a high-pass filter in temporal domain. We consider a moving window of T = 300 s, and in each time window we construct a detrended time series. On each time window, the detrended time series is used to evaluate the q-th–order structure function $S_q(\tau)$ considering as scales of interest those in the interval $\tau \in$ [1–40] s. The maximum scale investigated (40 s) is 10 times smaller than the size of the moving window (300 s) used; this ensures the reliable estimation of the 40 s fluctuation statistics. We suppose that the results obtained in the time domain are also valid for the spatial one. Under Taylor's frozen hypothesis the temporal scales can be related to the spatial scales, indeed formally, it assumes that the advection velocity of turbulence is much greater than the velocity scale of turbulence itself. Consequently, taking into account the orbital velocity of the Swarm satellite (∼7.6 km/s), the range of fluctuation scales τ corresponds to the range of spatial fluctuations between ∼8 km and ∼320 km. Thus, the findings of this type of analysis can describe the multi-scale structures and dynamics on meso-scale (10 s–100 s km). In the high-latitude ionosphere, the meso-scale covers a myriad of processes and phenomena, including polar cap patches, auroral arcs, streamers, diffusive aurora and field-aligned currents.

4. – Results

An example of the results that can be obtained by applying the q-th–order structure function, $S_q(\tau)$, analysis to the electron density data is reported in fig. 1. It shows the results obtained by analyzing 4 years of N_e data measured by the Swarm A satellite. In particular, the maps report the first- and second-order scaling exponent values at high latitudes in the Northern hemisphere. The coordinates are the magnetic latitude, ranging from 50° N to 90° N, and the magnetic local time (MLT). In this case, the whole dataset is considered, no subsampling are applied, which takes into account the geomagnetic and/or solar activity level. The obtained results show that the scaling properties of N_e fluctuations strongly depend on latitude and partially on magnetic local time. In general, at high latitudes the fluctuations have an anti-persistent character ($H < 0.5$) and a second-order scaling exponent value $\gamma(2) < 1$. Actually, in some locations $\gamma(2)$ is ∼0.66, which is the expected value in the case of a classic Kolmogorov's turbulence process. At lower latitudes, on the other hand, the N_e fluctuations exhibit different properties. They are persistent ($H > 0.5$) and have a second-order scaling exponent that is generally $\gamma(2) > 1$. The features of the analyzed scaling exponents can be summarized by observing that: 1) the Hurst exponent map shows how the different processes occurring inside and outside the auroral oval deeply influence the features of N_e fluctuations making them persistent and with a long correlation only outside the auroral region; 2) $\gamma(2)$ map reveals that N_e fluctuations are characterized by values of $\gamma(2) \sim 0.66$ inside the auroral oval, by slightly higher values along the boundary of the auroral oval, and even higher values equatorward the auroral oval; 3) inside the auroral oval, there are areas where N_e fluctuations show an anti-persistent character and contemporaneously a power spectral density with a spectral exponent $\beta \sim 5/3$. It is possible to suppose that turbulent processes are responsible for these peculiar features of N_e fluctuations. They could be ascribed to gradient drift and current convective instabilities in the case of a direct cascade process or to a Kelvin-Helmholtz instability in the case of an inverse

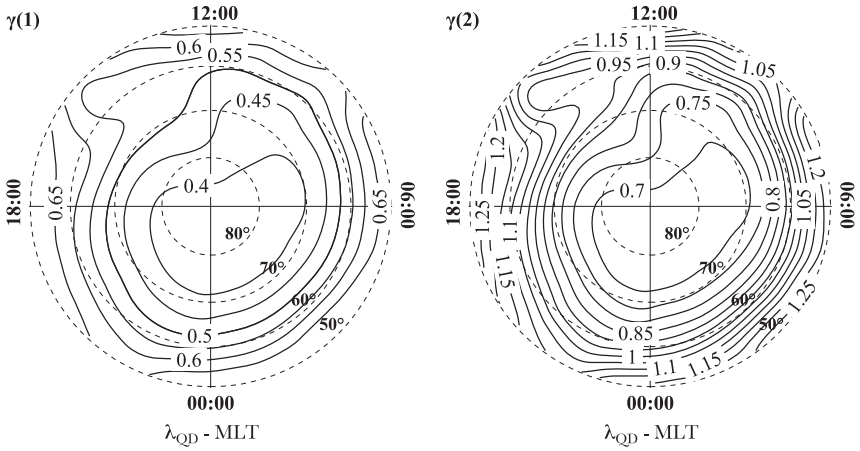

Fig. 1. – Polar view of the first- (Hurst exponent H) and second-order scaling exponent for the Northern hemisphere, in a QD-latitude ($\lambda_{QD} \leq 50°$ N) and MLT reference frame. Maps are drawn using data recorded onboard Swarm A from April 2014 to March 2018. Dashed circles indicate $\lambda_{QD} = 50°$, 60°, 70° and 80° N.

cascade [7]. However, the average obtained values for $\gamma(2)$, and consequently for β, are in the same range of values found by [17] in their statistical analysis of the ion density features in the high-latitude Northern hemisphere using DE2 satellite observations.

The dependence of the first- and second-order scaling exponent patterns on geomagnetic activity levels and on the interplanetary magnetic field (IMF) orientations has been investigated in previous papers [1-3, 18]. These studies have revealed that the distribution of N_e in the magnetic latitude – MLT plane is clearly modulated by the IMF orientations while the scaling properties of N_e fluctuations do not always show such a clear dependence on IMF orientations. It is not possible, for example, to recognize the expected dependence of the auroral oval extension on IMF orientations. Nevertheless, the average patterns of the two scaling exponents are not constant but slightly change with the IMF orientation change [2] as they tend to show a dependence on the level of geomagnetic activity [1, 3, 18]. The main result reported in fig. 1 is the existence of two families of N_e fluctuations. The first family is characterized by N_e fluctuations with a persistent character that are often associated with spectral exponents greater than 2. The second family is characterized by N_e fluctuations with an anti-persistent character and spectral exponents smaller than 2. This result, as confirmed by other previous studies [1-3, 18], is independent on the analyzed hemisphere, geomagnetic activity level and/or IMF orientation.

It has been found [1,3,4] that these two families are also characterized by different values of RODI, which is a proxy of the fluctuations intensity characterizing the ionospheric medium. This finding is reported in fig. 2, where the joint probability distributions between RODI and the first- and second-order scaling exponents respectively, have been evaluated considering the whole dataset. The family of N_e fluctuations characterized by anti-persistent character and an energy spectrum obeying a specific power-law scaling, which may suggest the existence of turbulent processes at their origin, is always associated with very high values of RODI. It has been shown [3] that this feature is independent of the geomagnetic activity level. Thus, among all the possible ionospheric irregularities, those due to turbulent processes seem to be always accompanied by plasma density variations stronger than those characterizing irregularities generated by different mechanisms.

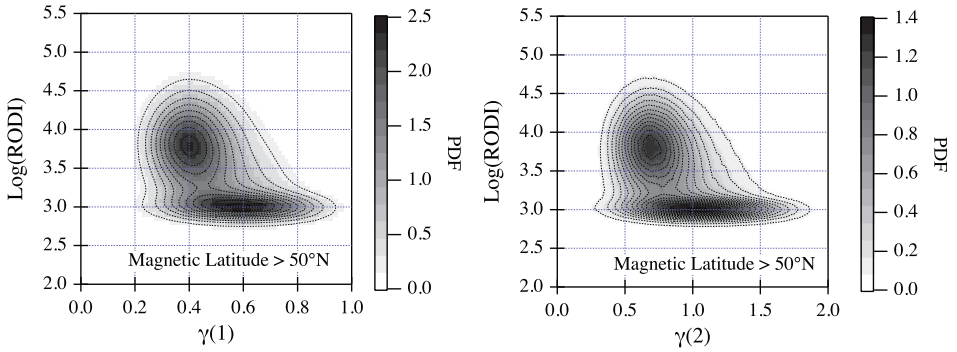

Fig. 2. – Joint probability distribution density functions at mid and high latitude in the Northern hemisphere between RODI and the first-order scaling exponent (left panel), and the second-order scaling exponent (right panel) obtained considering the whole dataset (from April 2014 to March 2018).

To study the existence of a possible link between the GPS signal loss and the scaling features of N_e fluctuations, the occurrence of loss of lock events recorded by Swarm A is evaluated [5]. By analyzing the geographical location of these events, at high latitude, it is possible to note that they mainly occur around the cusp region and along nightside auroral latitudes. These are also the regions identified in terms of families of electron density fluctuations characterized by anti-persistency ($H < 0.5$), a second-order scaling exponent $\gamma(2) < 1$, and high values of RODI (for more details, see [3]). This suggests that GPS signal loss events could be linked to the occurrence of turbulence processes characterizing the plasma density fluctuations and structures.

To verify this hypothesis, the values of RODI, first-, and second-order scaling exponents during the occurrence of LoL events at latitudes greater than 50° N have been evaluated. Successively, the joint probability density function of RODI and the first- and second-order scaling exponents conditioned to the occurrence of LoL have been computed. Figure 3 reports the joint probability density function of RODI and the second-order scaling exponent in correspondence with GPS LoL events. The obtained results show that during the GPS LoL events the electron density fluctuations are mainly characterized by a second-order scaling exponent value $\gamma(2) < 1$ and extremely high values of RODI ($>10^4\,\mathrm{cm}^{-3}\mathrm{s}^{-1}$). These events are also characterized by N_e fluctuations with an anti-persistent character (data are not shown). Thus, the occurrence of GPS LoL events seems to be associated with the family of irregularities characterized by values of scaling exponents that suggest the existence of turbulence phenomena. In addition, within this family an important proxy seems to be the RODI value. Log(RODI) > 4 seem to be associated with the occurrence of GPS malfunctions.

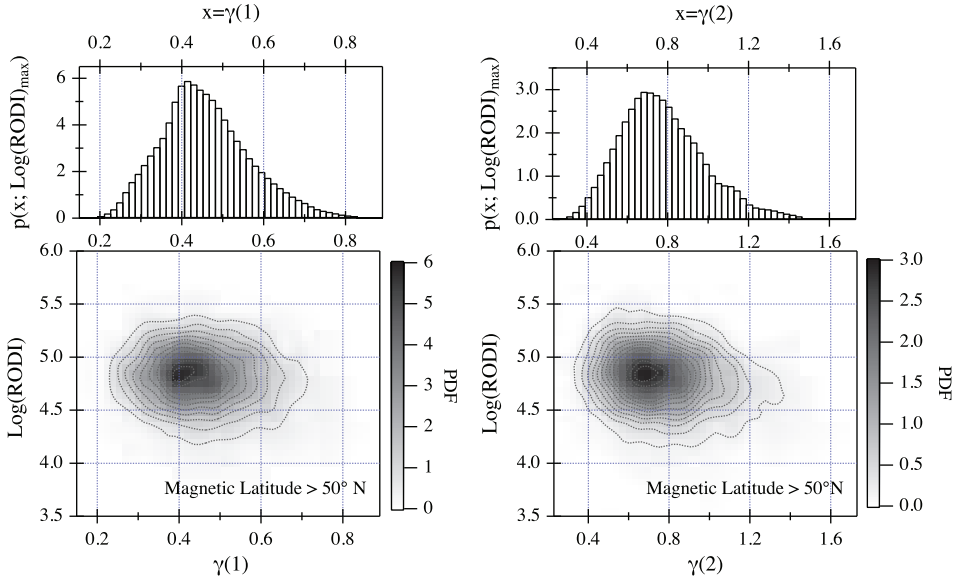

Fig. 3. – On the bottom: joint probability distribution density functions at mid and high latitude in the Northern hemisphere between RODI and $\gamma(1)$ (left panel) and $\gamma(2)$ (right panel), respectively conditioned to the occurrence of loss of lock events. On the top: probability distribution of $\gamma(1)$ (left panel), and $\gamma(2)$ (right panel) values at the maximum value of RODI.

5. – Summary and conclusions

Turbulence phenomena are at the origin of several important ionospheric dynamical processes. Since the mid-eighties, the ionospheric plasma turbulence has been the subject of several interesting papers (see for example [7]), the turbulent properties of electric [14,19-22] and magnetic fluctuations [15,16,22-24] observed at different altitudes and latitudes have been studied over the years. Great attention has also been paid to the role of turbulence in the generation and dynamics of ionospheric inhomogeneities and irregularities (see, *e.g.*, [18,25,26]). In the last few years, the role of turbulence processes in the ionosphere is becoming more and more important. It is understood that it can have a key role in the framework of space weather. Indeed, the ionospheric inhomogeneities and irregularities are among the main causes of disturbances in the propagation of electromagnetic signals in the ionosphere, and consequently a better understanding of the turbulence will be of help to all those systems, such as the GPS and GNSS, which are based on the propagation of electromagnetic signals through the ionosphere.

The INTENS project sought to answer some important questions like "Why are GPS signals sometimes weak or even absent? Why do these disturbances sometimes happen against all predictions? Why can not we predict the possible weakening or even loss of a GPS signal correctly?". The starting point is to become aware that not all ionospheric irregularities are equal. Different physical processes are at the basis of the generation and dynamics of ionospheric inhomogeneities and irregularities. Some of these irregularities are in a turbulent state. Indeed, a large number of instabilities typical of plasmas can feed fluctuations which then evolve into a power-law spectrum thanks to nonlinear interactions. It has been found that in the high-latitude ionosphere two different families of plasma density irregularities exist [1, 3]. They are characterized by different mean values of scaling exponents and RODI. The first family is characterized by antipersistency, $\gamma(2) < 1$, and high values of RODI. This family is mainly located inside the auroral oval, where particle precipitation dominates. This population could be due to turbulent mechanisms generated by gradient drift instability (GDI) or convective current instability. The observed average value of the spectral density exponent associated with this population is $\sim$1.7 and it is in agreement with previous findings [25, 27] and with theoretical predictions for this turbulent mechanism [7]. However, it is not possible to exclude that other mechanisms could be at the origin of the observed spectral features, as for instance the occurrence of coherent structures and nonlinear wave interactions [27], which are also a product of an intermittent turbulent cascade that is a common feature of strong turbulence. The second family is characterized by persistency, $\gamma(2) > 1$, and low values of RODI. It is mainly located at lower latitudes, outside the auroral oval [3]. The different processes inside plasma density irregularities are at the base of the occurrence of GPS loss of lock events. It has been found that when an electromagnetic signal travels cross plasma density irregularities characterized by turbulent processes, it can be reflected, refracted or completely absorbed. Indeed, the findings of this study show that the GPS loss of lock occurrences are associated with N_e fluctuations characterized by turbulent processes and accompanied by extremely high values of RODI. The obtained results are valid for electron density fluctuations at the meso-scale, indeed taking into account the time resolution of measurements (1 s) and the orbital velocity of the Swarm satellite, the analyzed range of spatial electron density fluctuations is between $\sim$8 km and $\sim$320 km. Extended opportunities to better investigate the scaling properties of electron density fluctuations at shorter spatial scales will be obtained with the future NanoMagSat mission for which continuous 2 kHz measurements will be acquired [28].

However, the obtained result paves the way for the realization of effective models for the prediction of the loss of lock and/or degradation of GPS signals in which for the first time the turbulence processes and the amplitude of ionospheric electron density fluctuations are taken into account. In the future, it would be interesting to explore the possibility to implement a high-latitude empirical model capable of reproducing the regions where, according to both values of RODI and scaling exponents of the electron density fluctuations, there are the physical conditions for the occurrence of disturbances potentially harmful to the propagation of radio signals. This empirical model, extremely useful for practical applications, would provide maps of risk in terms of the occurrence of high-amplitude turbulent phenomena linked to GPS loss of lock events. Obviously, these maps should depend on different factors, and they should be parameterized according to different physical quantities such as: the interplanetary magnetic field orientation, the dipole tilt angle, the solar and geomagnetic activity level, and so on. In this way, after setting specified driving conditions, it would be possible to know the position at high latitude in the Northern and Southern hemispheres of those regions where the features of electron density fluctuations can potentially disturb the propagation of radio signals. A preliminary model will be implemented as part of the SPIRiT (Space weather in Polar Ionosphere: the Role of Turbulence) project funded by the Italian PNRA (Programma Nazionale di Ricerche in Antartide) in the next years.

* * *

The author acknowledges the financial support from the European Space Agency (ESA contract No. 4000125663/18/I-NB-EO Science for Society Permanently Open Call for Proposals EOEP-5 BLOCK4 (INTENS)) and from the Italian PNRA under contract PNRA18-00289-A "Space weather in Polar Ionosphere: the Role of Turbulence". The author acknowledges all the members of the INTENS and SPIRiT teams for the work they did and their commitment to the success of the projects.

REFERENCES

[1] De Michelis P., Pignalberi A., Consolini G., Coco I., Tozzi R., Pezzopane M., Giannattasio F. and Balasis G., *J. Geophys. Res. Space Phys.*, **125** (2020) e2020JA027934.
[2] Consolini G., Tozzi R., De Michelis P., Coco I., Giannattasio F., Pezzopane M., Marcucci M. F. and Balasis G., *J. Atmos. Sol. Terr. Phys.*, **217** (2021) 105531.
[3] De Michelis P., Consolini G., Pignalberi A., Tozzi R., Coco I., Giannattasio F., Pezzopane M. and Balasis G., *Sci. Rep.*, **11** (2021) 6183.
[4] De Michelis P., Consolini G., Tozzi R., Pignalberi A., Pezzopane M., Coco I., Giannattasio F. and Marcucci M. F., *Remote Sens.*, **13** (2021) 759.
[5] Pezzopane M., Pignalberi A., Coco I., Consolini G., De Michelis P., Giannattasio F., Marcucci M. F. and Tozzi R., *Remote Sens.*, **12** (2021) 2209.
[6] Tsunoda R. T., *Rev. Geophys.*, **26** (1988) 719.
[7] Kintner P. M. jr. and Seyler C. E., *Space Sci. Rev.*, **41** (1985) 91.
[8] Knudsen D. J., Burchill J. K., Buchert S. C., Eriksson A. I., Gill R., Wahlund J.-E., Ahlen L., Smith M. and Moffat B., *J. Geophys. Res. Space Phys.*, **122** (2017) 2655.
[9] Jin Y., Spicher A., Xiong C., Clausen L. B. N., Kervalishvili G., Stolle C. and Miloch W. J., *J. Geophys. Res. Space Phys.*, **124** (2019) 1262.
[10] Pignalberi A., *Comput. Geosci.*, **148** (2021) 104675.
[11] Van den IJssel J., Forte B. and Montenbruck O., *Earth Planets Space*, **68** (2016) 85.

[12] Noja M., Stolle C., Park J. and Luhr H., *Radio Sci.*, **48** (2013) 289.
[13] Hurst H., *ICE Proc.*, **5** (1956) 519.
[14] Weimer D. R., Goertz C. K. and Gurnett D. A., *J. Geophys. Res.*, **90** (1985) 7479.
[15] De Michelis P., Consolini G. and Tozzi R., *Geophys. Res. Lett.*, **42** (2015) 3100.
[16] De Michelis P., Consolini G., Tozzi R. and Marcucci M. F., *J. Geophys. Res. Space Phys.*, **122** (2017) 10548.
[17] Kivanc Ö. and Heelis R. A., *J. Geophys. Res.*, **103** (1998) 6955.
[18] Giannattasio F., De Michelis P., Consolini G., Quattrociocchi V., Coco I. and Tozzi R., *Ann. Geophys.*, **62** (2019) M453.
[19] Golovchanskaya I. V. and Kozelov B. V., *J. Geophys. Res.*, **115** (2010) A09321.
[20] Heppner J. P., Liebrecht M. C., Maynard N. C. and Pfaff R. F., *J. Geophys. Res.*, **98** (1993) 1629.
[21] Tam S., Chang W. Y., Kintner P. M. and Klatt E., *Geophys. Res. Lett.*, **32** (2005) L05109.
[22] Kozelov B. V. and Golovchanskaya I. V., *Geophys. Res. Lett.*, **33** (2006) L20109.
[23] De Michelis P., Consolini G., Tozzi R., Giannattasio F., Quattrociocchi V. and Coco I., *Ann. Geophys.*, **62** (2019) GM449.
[24] Golovchanskaya I. V., Ostapenko A. A. and Kozelov B. V., *J. Geophys. Res.*, **111** (2006) A12301.
[25] Basu S., Basu S., MacKenzie E., Fougere P. F., Coley W. R., Maynard N. C. *et al.*, *J. Geophys. Res.*, **93** (1988) 115.
[26] Earle G. D., Kelley M. C. and Ganguli G., *J. Geophys. Res.*, **94** (1989) 15321.
[27] Spicher A., Miloch W. J., Clausen L. B. N. and Moen J. I., *J. Geophys. Res.*, **120** (2015) 10959.
[28] Hulot G. *et al.*, *Nanosatellite High-Precision Magnetic Missions Enabled by Advances in a Stand-Alone Scalar/Vector Absolute Magnetometer*, in *IGARSS 2018 - 2018 IEEE International Geoscience and Remote Sensing Symposium* (IEEE) 2018, pp. 6320–6323, https://doi.org/10.1109/IGARSS.2018.8517754.